

Improving retrieval quality for airborne limb sounders by horizontal regularisation

J. Ungermann^{1,2}

¹Institute for Energy and Climate Research - Stratosphere, Research Centre Jülich, Germany

²National Center for Atmospheric Research, Boulder, Colorado, USA

Abstract. Modern airborne infrared limb sounders are capable of measuring profiles so fast that neighbouring profiles are very similar to one another. This can be exploited by **retrieving whole 2-D cross-sections** instead of simple 1-D profiles.

This poster presents algorithms that are able to perform such a large-scale retrieval and that **efficiently produce typical diagnostic quantities**. The characteristics and capabilities of the proposed method are analysed and demonstrated in a detailed case study using a series of profiles that were measured by CRISTA-NF (Cryogenic Infrared Spectrometers and Telescope for the Atmosphere–New Frontiers).

It is shown that cross-section retrievals can **either reduce noise-induced artefacts** or **produce finer vertical structures** while maintaining the same image noise level. This technique can also be applied to improve the retrievals for other instrument types including current satellite-borne nadir-sounders and near future satellite-borne limb sounders.

Retrieval and Monte Carlo Diagnostics

The cross-section retrieval works similar to a typical profile retrieval. The major principal differences are in the implementation of the atmospheric representation and the setup of regularization. Further, due to the increased problem size, other algorithms must be employed to solve the basic equations. The solution is iteratively derived by

$$\mathbf{x}_{i+1} = \mathbf{x}_i - \left(\mathbf{S}_a^{-1} + \mathbf{F}'(\mathbf{x}_i)^T \mathbf{S}_\epsilon^{-1} \mathbf{F}'(\mathbf{x}_i) + \lambda_i \mathbf{I}_n \right)^{-1} \cdot \left(\mathbf{S}_a^{-1} (\mathbf{x}_i - \mathbf{x}_a) + \mathbf{F}'(\mathbf{x}_i)^T \mathbf{S}_\epsilon^{-1} (\mathbf{F}(\mathbf{x}_i) - \mathbf{y}) \right).$$

Sparse representations are a necessity, especially for the regularization matrix:

$$\mathbf{S}_a^{-1} = (\alpha_0)^2 \mathbf{L}_0^T \mathbf{L}_0 + (\alpha_1^v)^2 \mathbf{L}_1^v T \mathbf{L}_1^v + (\alpha_1^h)^2 \mathbf{L}_1^h T \mathbf{L}_1^h$$

For the autoregressive form of a two-dimensional covariance matrix,

$$(\mathbf{S})_{i,j} = \sigma_i \sigma_j e^{-\frac{|v_i - v_j|}{c_v}} e^{-\frac{|h_i - h_j|}{c_h}}$$

exists also a closed form to directly setup its inverse, which is exploited for the two-dimensional diagnostics (see reference below). The gain matrix (or just its individual rows \mathbf{g}_i) can be calculated to derive the effect of, e.g., background gases on the solution:

$$(\sigma_i^{\text{gas}})^2 = \mathbf{g}_i^T \mathbf{F}'_{\text{gas}}(\mathbf{x}_f)^T \mathbf{z}, \text{ with } \mathbf{S}_{\text{gas}}^{-1} \mathbf{z} = \mathbf{F}'_{\text{gas}}(\mathbf{x}_f) \mathbf{g}_i$$

As the calculation for the whole gain matrix is tedious, a more efficient way of deriving error estimates is to randomly perturb the measurements according to the assumed error characteristics and derive for many perturbations the perturbed retrieval result:

$$\mathbf{x}_i^{\text{mc}} = \mathbf{x}_f - \left(\mathbf{S}_a^{-1} + \mathbf{F}'(\mathbf{x}_f)^T \mathbf{S}_\epsilon^{-1} \mathbf{F}'(\mathbf{x}_f) \right)^{-1} \cdot \left(\mathbf{F}'(\mathbf{x}_f)^T \mathbf{S}_\epsilon^{-1} \boldsymbol{\epsilon}_i^{\text{mc}} \right).$$

The standard deviations of these linear solutions gives the desired error estimate. To derive the total error, it is advantageous to construct error vectors summing over all known error sources.

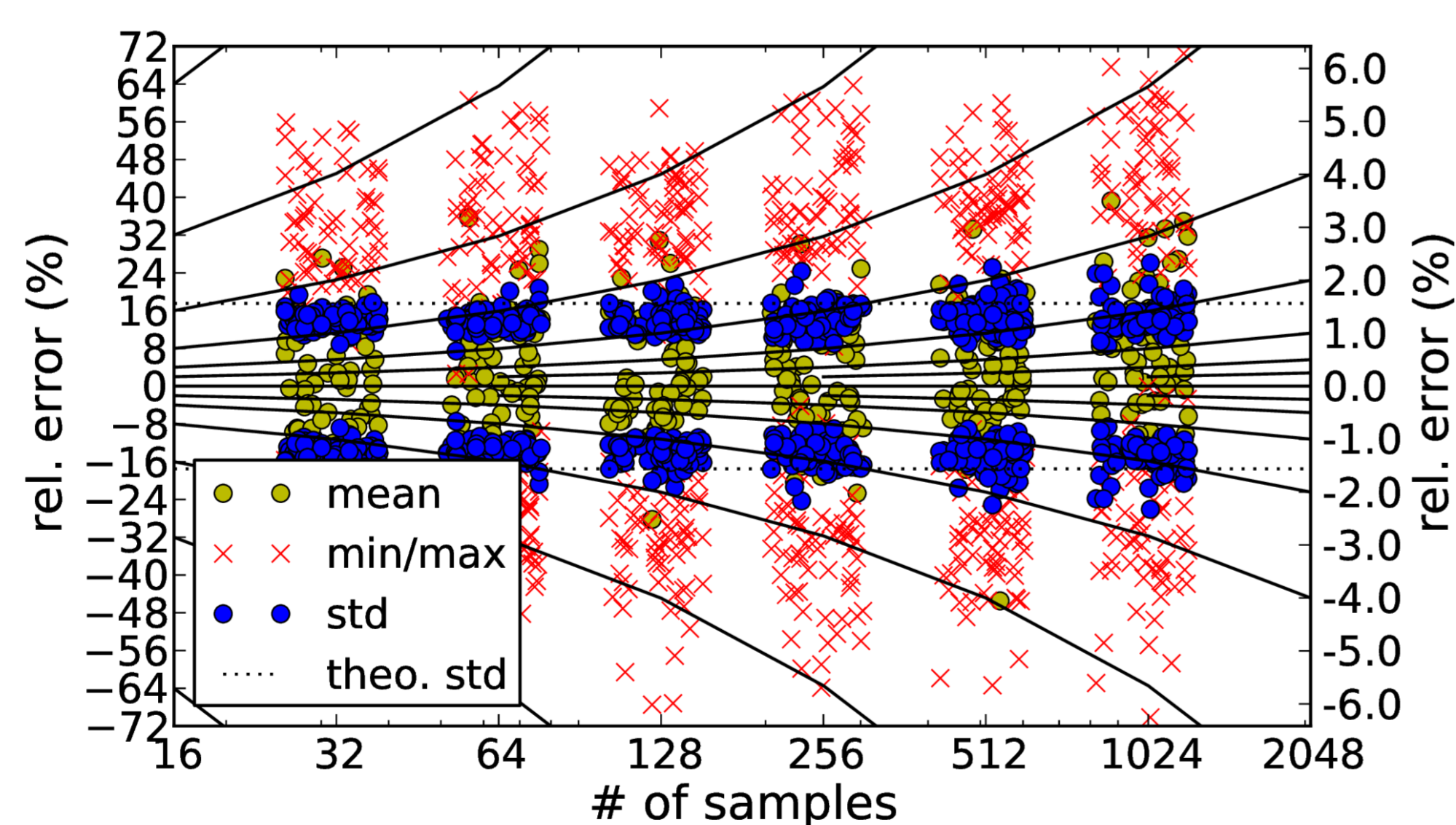


Fig. 1. Precision of error estimate for different number of samples.

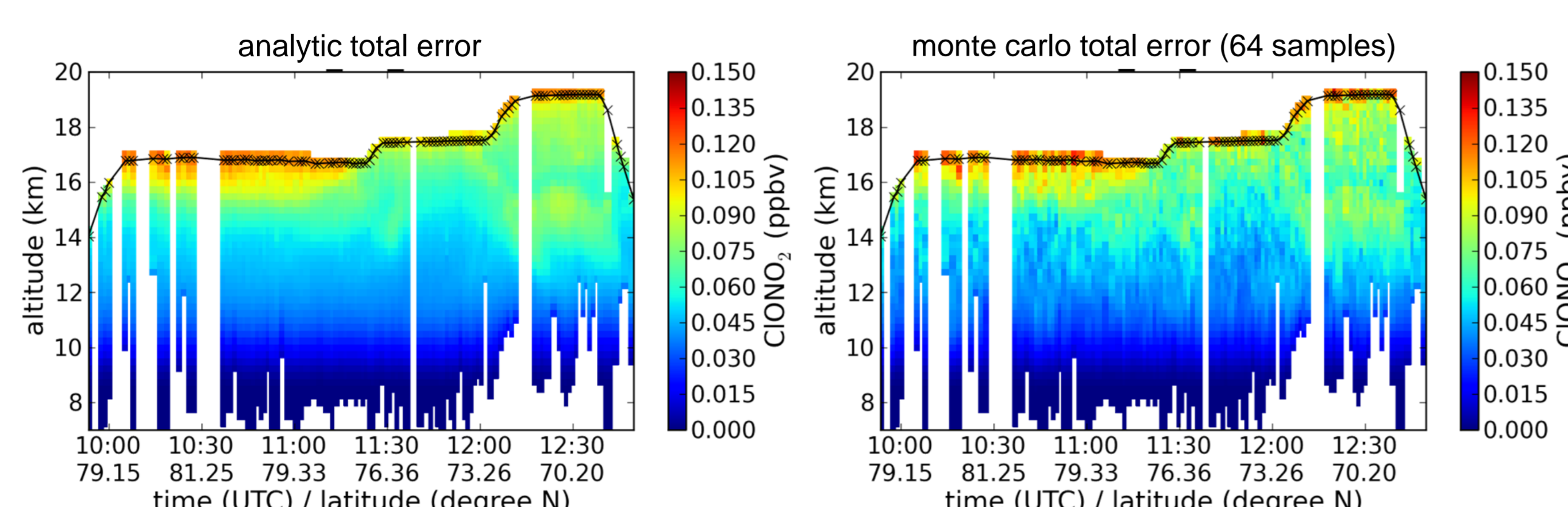


Fig. 2. Example of total error for a cross-section retrieval with 93870 unknowns determined by exact calculation (left, 500 hours computation time per target) and estimation with 64 samples (right, 1 hour computation time for all 11 targets).

Horizontal regularisation

Adding horizontal constraints allows to reduce the noise with an acceptable effect on the horizontal resolution.

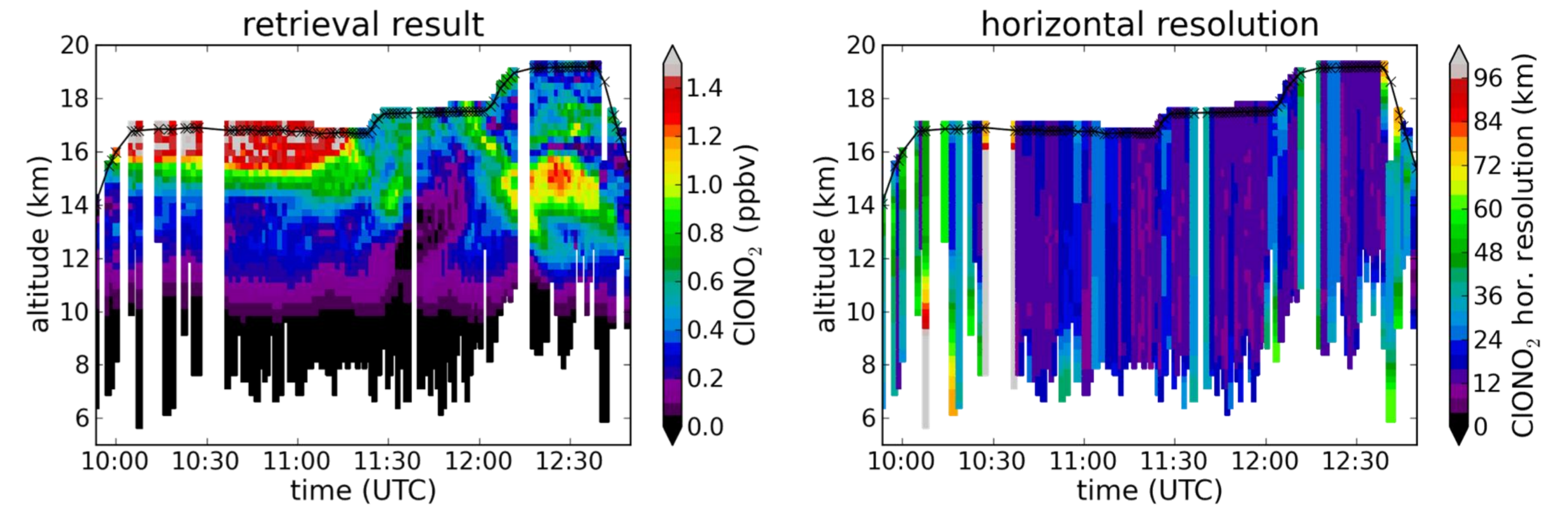


Fig. 3. CIONO₂ volume mixing ratios and horizontal resolutions, respectively, for the standard vertical regularisation and no horizontal regularisation.

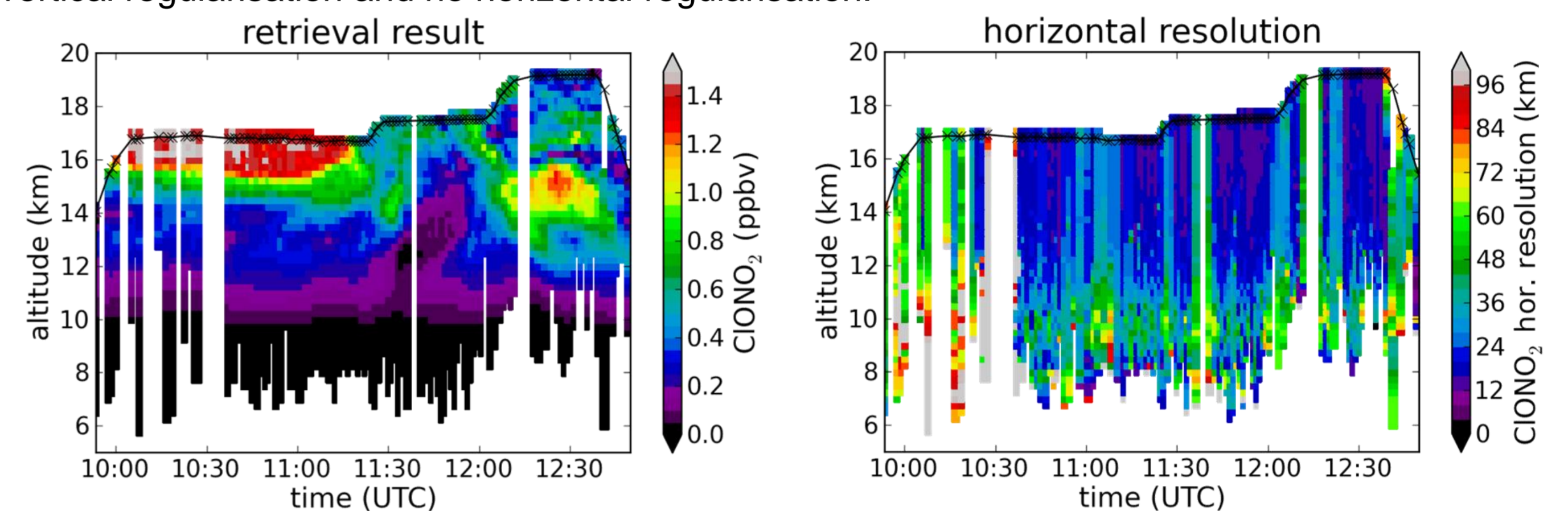


Fig. 4. CIONO₂ volume mixing ratios and horizontal resolutions, respectively, for the standard vertical regularisation and horizontal regularisation 200 times as strong as the vertical one.

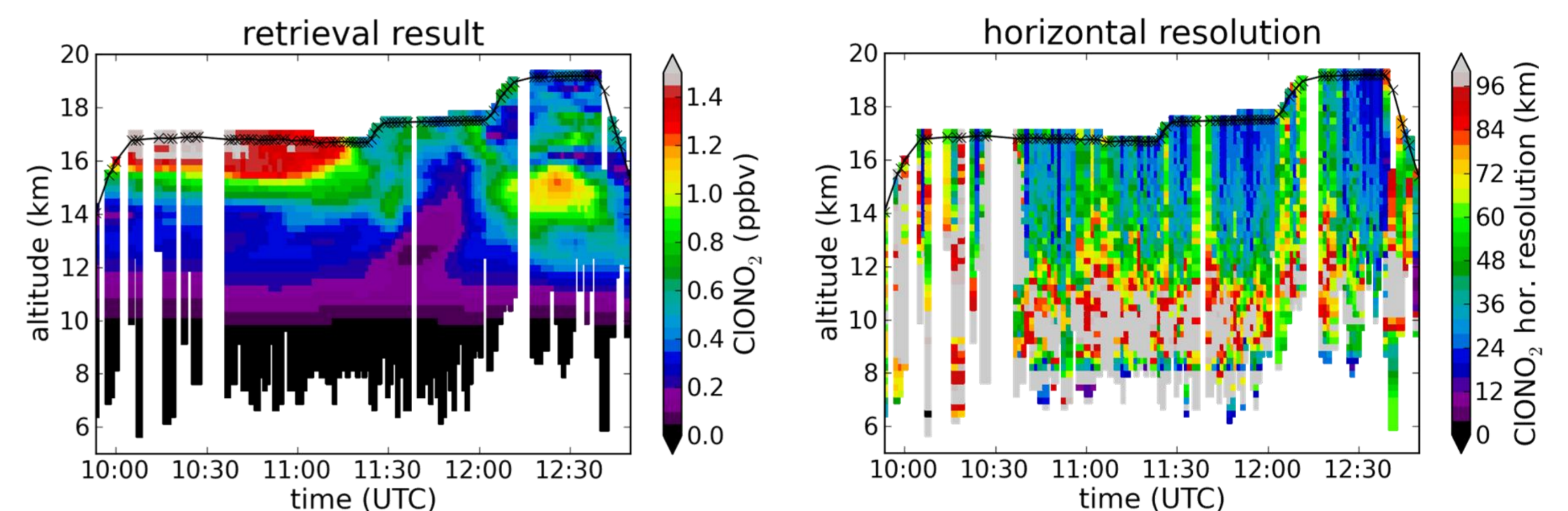


Fig. 5. CIONO₂ volume mixing ratios and horizontal resolutions, respectively, for the standard vertical regularisation and horizontal regularisation 2000 times as strong as the vertical one.

Increasing the vertical resolution

Using horizontal regularisation, the vertical resolution can be improved without increasing the error by stochastic error sources.

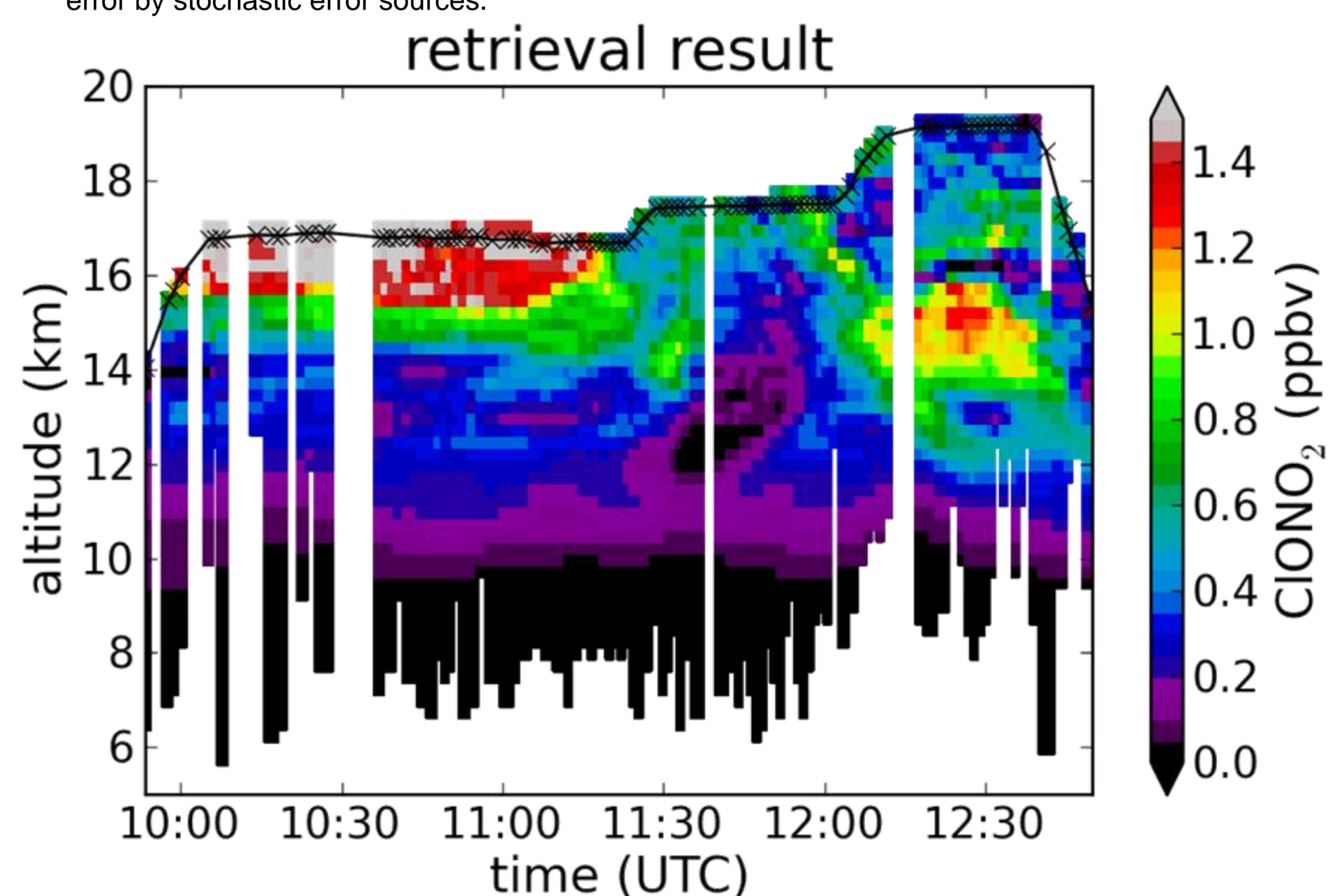


Fig. 6. CIONO₂ volume mixing ratios for a tenth of the standard vertical regularisation and horizontal regularisation 200 times as strong as the standard vertical strength.

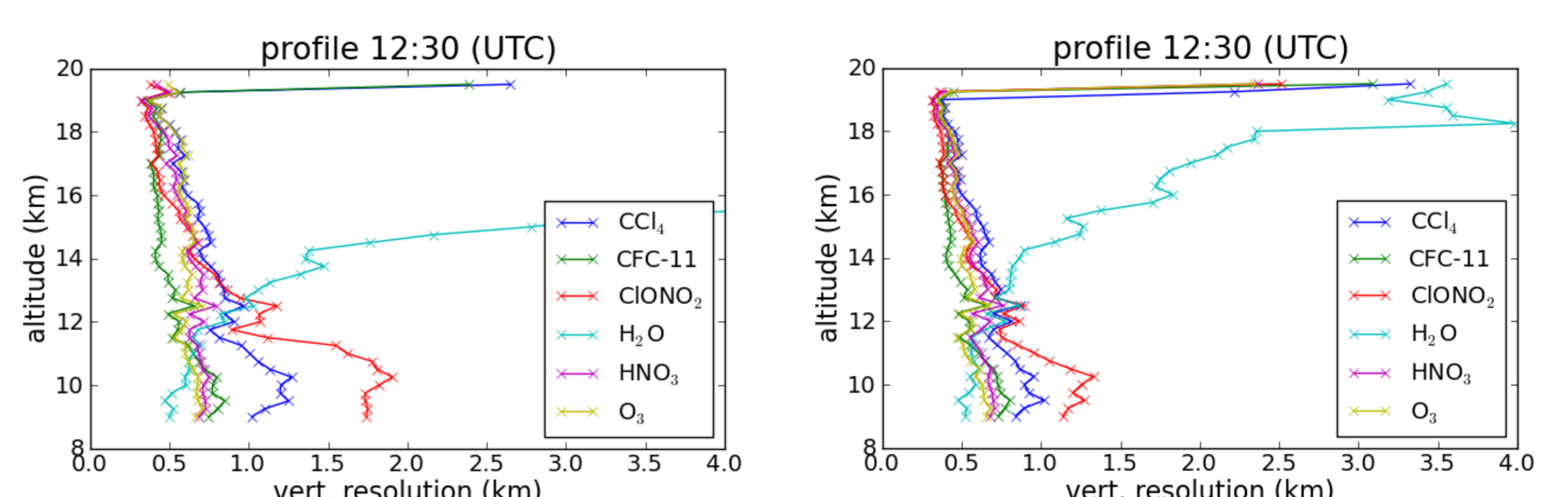


Fig. 7. Vertical resolution for the standard setup with no horizontal regularisation and the improved one with decreased vertical and added horizontal regularisation.